

## Effect of pH on the Structural Properties of Electrodeposited Nanocrystalline FeCo Films

Wei Lu<sup>1,\*,\*\*</sup>, Caiwen Ou<sup>2,\*,\*\*</sup>, Ping Huang<sup>1</sup>, Pengfei Yan<sup>1</sup>, and Biao Yan<sup>1</sup>

<sup>1</sup> School of Materials Science and Engineering, Shanghai Key Lab. of D&A for Metal-Functional Materials, Tongji University, Shanghai 200092, China

<sup>2</sup> Southern Medical University, No.1023, Shatai Nan Road, Guangzhou City, Guangzhou 510515, China

\*E-mail: [1284572007@qq.com](mailto:1284572007@qq.com); [weilu@tongji.edu.cn](mailto:weilu@tongji.edu.cn)

\*\* These authors made equal contributions to this work.

Received: 9 April 2013 / Accepted: 16 May 2013 / Published: 1 June 2013

---

In this paper, the effect of electrolyte pH on the composition and microstructure of FeCo films were investigated in details by using EDS, XRD and SEM. The composition of FeCo films is greatly affected by the electrolyte pH. With increasing temperature, the Fe content is increased while Co content is decreased. Low electrolyte pH ( $\leq 3$ ) favors the formation of fcc  $\gamma$  phase while high electrolyte pH (4 and 5) leads to the formation of bcc  $\alpha$ -Co<sub>7</sub>Fe<sub>3</sub> phase in the studied films. High electrolyte pH results in a small decrease in the lattice parameter for the fcc phase and a small increase for that of bcc phase. With increasing pH value, the averaged grain sizes of fcc phase and bcc phase increase. The films prepared at low pH values (1 and 2) shows a very poor quality with rough surface. The surfaces of the films electrodeposited at high pH value (3~5) are generally quite smooth, uniform and compact. And porous and cracks can be observed in the FeCo films electrodeposited at high pH value (3~5).

---

**Keywords:** FeCo film; electrochemical deposition; electrolyte pH

### 1. INTRODUCTION

FeCo alloys have been extensively studied as soft magnetic materials due to their good properties. They have been used widely and commercially in magnetic sensors, magnetic recording head, motors, and generators in electric vehicles since it has high Curie temperature, high magnetization, low coercivity, low hysteresis loss, low eddy current loss, high electric permeability and good thermal stability.[1-3]

Electrodeposition of FeCo alloy films is one of the most popular fabrication processes for its low cost and simple, flexible operation, inexpensive apparatus and easy reliable control by changing the parameters in the whole electrodeposition process although stable plating baths are needed for commercial processing. In electrodeposition, the growth mechanism, morphology, and microstructural properties of the film depend on electrodeposition conditions such as electrolyte pH, temperature, deposition potential and electrolyte composition. The variations of these parameters have been shown to affect the growth mechanism, morphology, microstructure, and magnetic properties of the deposited films [4–14]. By adjusting these deposition parameters, it can be possible to control and optimize the structural, mechanical, magnetic and magneto-transport properties of electrodeposited films. Generally, the aim of the work is to clarify the effect of deposition conditions on electrodeposited FeCo films. It is well established that the variation of current density produces a variation in grain size, due to the occurrence of hydrogen evolution at the cathode interface. A variation of this hydrogen evolution reaction that occurred at the cathode surface caused the modification of the growth interface and consequently the change of the surface energy and growth process which in order conducted the formation of larger grain size [15-19]. Also, the bath temperature in electrodeposition solutions is extremely important due to their influence on the nucleation-growth and microstructure of the resulting deposits. It is well known that bath temperature affect the physical and mechanical properties of electrodeposited thin films such as surface roughness, grain size, texture, brightness, internal stress, current efficiency, and even chemical composition [18-24]. In addition, it was observed that the solution pH changes the condition of metal ions, which usually plays a key role to control the film properties [23-28]. A modification of bath pH can also affect the crystallite size and consequently the magnetic properties such as magnetoresistance of some materials obtained by electrodeposition [23-28]. Consequently, the electrolyte pH is one of critical parameters to achieve the desired structural and functional properties.

In this paper, a detailed study of the electrolyte pH effect on the microstructural properties of FeCo alloy films is presented. We have shown that the composition, phase structure, grain size, lattice parameter and morphology of FeCo films were significantly affected by the pH of electrolytes. The work might be useful to understand better how electrolyte pH affects the properties of electrodeposited films.

## 2. EXPERIMENTAL

FeCo thin films were fabricated by electrochemical deposition from sulfate bath using a conventional three electrode cell. The copper plate serves as the working cathode with the surface area of  $1\text{cm}^2$  while a graphite plate serves as the anode with much larger surface area. Prior to deposition, the substrate was first mechanically polished, then washed in 10%  $\text{H}_2\text{SO}_4$  and distilled water. The reference electrode was a saturated calomel electrode.

The compositions of the electrolytes of  $\text{Co}^{2+}/\text{Fe}^{2+}$  were shown in Table 1, together with major electrodepositing parameters. The total concentration of ferrous sulfate [ $\text{FeSO}_4 \cdot 7\text{H}_2\text{O}$ ] and cobalt sulfate [ $\text{CoSO}_4 \cdot 7\text{H}_2\text{O}$ ] was kept 0.35 mol/L. All chemicals were reagent grade and dissolved in

distilled water. The electrodeposition was conducted at different electrolyte pH (1~5) with a certain stirring rate.

The crystallographic structure of electrodeposited FeCo films was characterized by X-ray Diffraction (XRD). The compositions of the samples were detected through energy dispersive spectrometer (EDS). Field-emission scanning electronic microscopy (FESEM) was employed to examine the morphology of the films.

**Table 1.** Compositions of the electrolytes and major electrodepositing parameters

Composition	Temperature (°C)	Current density (mA/cm <sup>2</sup> )
CoSO <sub>4</sub> ·7H <sub>2</sub> O (0.2mol/L)	25	10
FeSO <sub>4</sub> ·7H <sub>2</sub> O (0.15mol/L)		
Na <sub>2</sub> SO <sub>4</sub> (0.7mol/L)		
Ascorbic Acid (0.05mol/L)		
Boric acid (0.4mol/L)		

### 3. RESULTS AND DISCUSSION

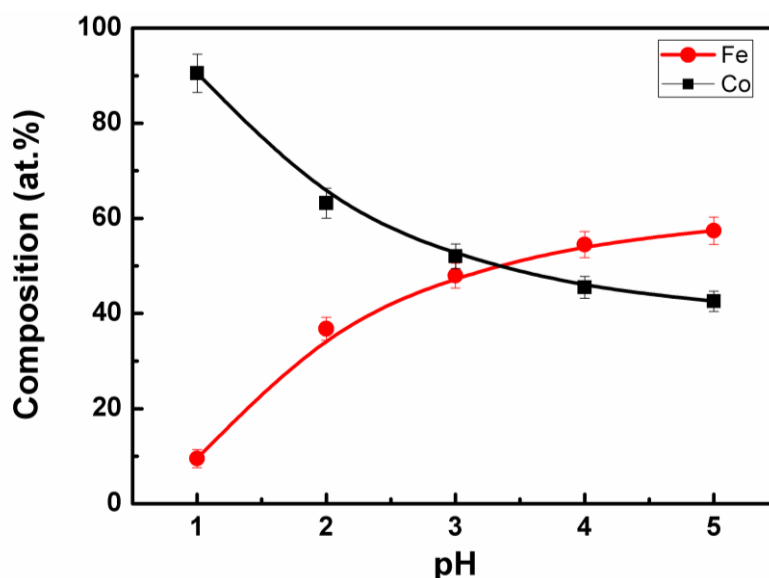


**Figure 1.** Composition of co-electrodeposited FeCo alloy films at different electrolyte pH

The content of Fe and Co of the FeCo films was measured by energy dispersive analysis of X-ray spectroscopy. Fig.1 shows the dependence of deposit compositions on various electrolyte pH values in the electrodeposition of FeCo thin films. As can be seen, the Fe concentration in the co-deposited films is increased from around 10 at.% to 57 at.% when the electrolyte pH value is increased from 1 to 5. The molar ratio of Co:Fe in the bath solution was 4:3, which should result in electrodeposited films with compositions of ~43 at% Fe (~57 at% Co) assuming non-preferential co-

electrodeposition. Thus, it can be suggested that Co is preferentially deposited when the electrolyte pH value is set as 1, relative to the composition of electrolyte solution, at the expense of Fe. The behavior is as normally expected since the more noble metal (Co) is deposited preferentially. Therefore, the results indicate a normal co-electrodepositing behavior for the electrolyte solution at pH=1.

The electrodeposition process is mainly dominated by three factors [29]: (1) The dissolution of the freshly deposited metal atoms on the substrate because of the acid circumstance in the electrolyte; (2) The formation and absorption of metals hydroxides on the electrode surface; (3) The normal electrodeposition of the metals. A lower pH value favors the dissolution of freshly deposited metal and depresses the formation and absorption of metal hydroxides. The process is predominated by the normal deposition of the metal, resulting in lower iron content in the coatings due to a lower reduction potential of iron.

Nevertheless, a higher pH value favors the formation and absorption of metal hydroxides and depresses the dissolution of the freshly deposited metal. When the electrolyte pH value is increased to 2~3, the composition of the deposits roughly reflects the solution composition, while at pH value higher than 4, the deposited films become Fe-rich. The results indicate an anomalous co-electrodepositing behavior for the electrolyte solution at high pH value. This so-called anomalous co-deposition has long been reported [30-32]. A hydroxide-based model for the anomalous co-deposition was first proposed by Dahms and Croll [33]. This model was modified later by emphasizing the role of ionized hydrolysis products [34, 35]. Recent researches indicated that the electrode kinetics, such as the adsorption of monovalent ions intermediates on the electrode, plays a more important role than the chemical reactions in the solution and it is thought to be the result of an inhibiting effect of Fe on the nucleation and growth of Co on the cathode surface. [36-38]

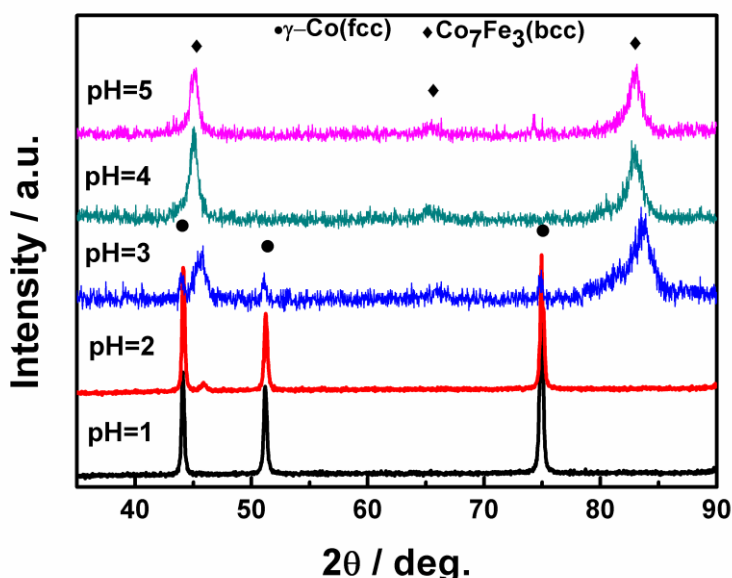


**Figure 2.** XRD patterns of FeCo films electrodeposited at different electrolyte pH values

Concerning a successful application of the electrodeposited FeCo alloys, not only the composition but also the microstructure has to be controlled precisely. One of the most important

microstructure issues is the phase structure, since both the superior magnetic and mechanical properties depend strongly on it. Fig.2 shows the XRD patterns of FeCo films electrodeposited at different electrolyte pH value. From the patterns, it can be seen that the films have a mixed phases of face-centered cubic (fcc) solid solution ( $\gamma$  phase) and body-centered cubic (bcc)  $\alpha$ -Co<sub>7</sub>Fe<sub>3</sub> phase ( $\alpha$ -Fe type). As seen from the figure, the reflections from the characteristic (111), (200) and (220) crystal planes of fcc CoFe solid solution phase were observed at approximately  $2\theta=44^\circ$ ,  $51^\circ$  and  $75^\circ$ , respectively. In addition, the (110), (200), (211) peaks of bcc  $\alpha$ -Co<sub>7</sub>Fe<sub>3</sub> phase were observed at about  $45^\circ$ ,  $66^\circ$  and  $84^\circ$ , respectively. The patterns indicate that the film electrodeposited at pH=1 has a single phase of fcc phase. When the electrolyte pH is increased to 2, the (110) peak of bcc phase appears but the intensity is relatively very weak. Further increase the electrolyte pH to 3, the peak intensity of bcc phase increases sharply. This means that the fcc phase transforms to bcc phase and the bcc phase becomes dominant in the FeCo film. The structure becomes completely bcc for the FeCo films when the electrolyte pH value is increase to 4~5, as seen from Fig. 2. Results indicate that a two-phase mixed structure of the fcc phase and the bcc solid solution phase forms for intermediate conditions (pH=2~3).

According to the phase diagram of Fe-Co binary alloy [39], fcc solid solution phase is thermodynamically stable for high Co concentration ( $>90$  at%) at low temperature ( $<700^\circ\text{C}$ ) or for all alloy concentrations at temperatures between  $\sim 985^\circ\text{C}$  and  $\sim 1475^\circ\text{C}$  while bcc  $\alpha$  phase is stable for Fe concentrations in excess of 80 at% at temperatures below  $500^\circ\text{C}$ . The binary phase diagram gives a good indication of the phases that might be expected in Fe-Co thin films at a particular composition. However, although thermodynamically stable at low temperature and over a wide composition range (25~75 at% Fe) according to the phase diagram, the  $\alpha'$  phase is never observed in our electrodeposited thin films and other researches [2, 3, 40-42]. It is reported [2, 3, 40-42] that under many electrodeposition conditions the fcc Fe-Co solid solution phase and bcc  $\alpha$  phase form during electrodeposition. The formation of non-equilibrium phases of the two solid solution phases is not surprising for electrodeposition systems as the deposition rates do not provide sufficient time for the ordering of Co and Fe atoms on specific lattice positions to form  $\alpha'$ -CoFe phase. In our work, for electrodeposition of FeCo films with Co concentrations ranging from around 90 to 43 at% at all electrolyte pH values, the fcc solid solution was only detected for the electrolyte pH of low values (less than 3) while the bcc phase was obtained at high electrolyte pH values (higher than 3).

The lattice parameters of fcc and bcc phase in the electrodeposited FeCo films were calculated based on the peak positions in the XRD patterns. Table.2 shows the average lattice parameters of fcc and bcc phase in alloy films fabricated at different electrolyte pH. Higher depositing electrolyte pH leads to a small decrease in the lattice parameter for the bcc phase. This is to be expected due to the slightly smaller atomic radius of the Co atoms and enrichment of Co content in bcc phase. As can be seen from Fig.2, when the electrolyte pH increases from 1 to 3, the fcc  $\gamma$  Co phase transforms to bcc Co<sub>7</sub>Fe<sub>3</sub> phase and the Co<sub>7</sub>Fe<sub>3</sub> phase becomes dominant in the FeCo film. This means that more Fe atoms were involved in the formation of Co<sub>7</sub>Fe<sub>3</sub> and the content of Fe in the fcc  $\gamma$  Co solid solution was decreased with increasing electrolyte pH (1 to 3). The incorporation of small atoms into the lattice of the film would shrink the lattice and decrease the lattice parameters. In addition, the lattice parameter of the bcc Co<sub>7</sub>Fe<sub>3</sub> phase increases when the electrolyte pH is increased. This is caused by

the increasing Fe content in the FeCo film and more Fe atoms were involved in the formation of  $\text{Co}_7\text{Fe}_3$  phase when the electrolyte pH was increased from 2 to 5.

**Table 2.** Average lattice parameters (nm) of bcc phase and fcc phase in FeCo films prepared at different electrolyte pH

phase	pH				
	1	2	3	4	5
$\gamma$ Co(220)	0.3604	0.3599	0.3587	-	-
$\text{Co}_7\text{Fe}_3$ (110)	-	0.2798	0.2830	0.2856	0.2860

By using Scherer equation, the averaged grain sizes of  $\gamma$  Co phase in FeCo films electrodeposited at different electrolyte pH values are calculated and shown in Table 3. It can be seen that with increasing pH values, the averaged grain sizes of fcc phase increase from around 47 nm (pH=1) to 62 nm (pH=3). When the pH value is increased from 2 to 5, the averaged grain size of bcc phase increases slowly from around 22 nm (pH=2) to 32 nm (pH=5).

**Table 3.** Average grain sizes (nm) of bcc phase and fcc phase in FeCo films prepared at different electrolyte pH

phase	pH				
	1	2	3	4	5
$\gamma$ Co	46.8	60	61.8	-	-
$\text{Co}_7\text{Fe}_3$	-	21.8	23.9	27.86	31.99

Fig. 3 shows the surface morphology of FeCo films electrodeposited at various electrolyte pH values. The surface morphology is strongly influenced by the electrolyte pH. The films prepared at low pH values (1 and 2) shows a very poor quality with rough surface. The films are very thin (according to cross-section SEM images which are not shown here) and not uniform. This is mainly caused by the relatively low current efficiency and high hydrogen evolution during electrodepositing at low pH values. With increasing pH values (3 to 5), the surfaces of the electrodeposited films are generally smooth, uniform and compact because of the weakening of hydrogen evolution at higher pH values. But voids, pores and cracks are observed at higher pH values. At higher pH value (3~5), the deposition rate becomes larger with the increase of the pH due to the high current efficiency. The higher deposition rate causes a situation that there is no enough time for internal stress release and cracking of the coatings may occur

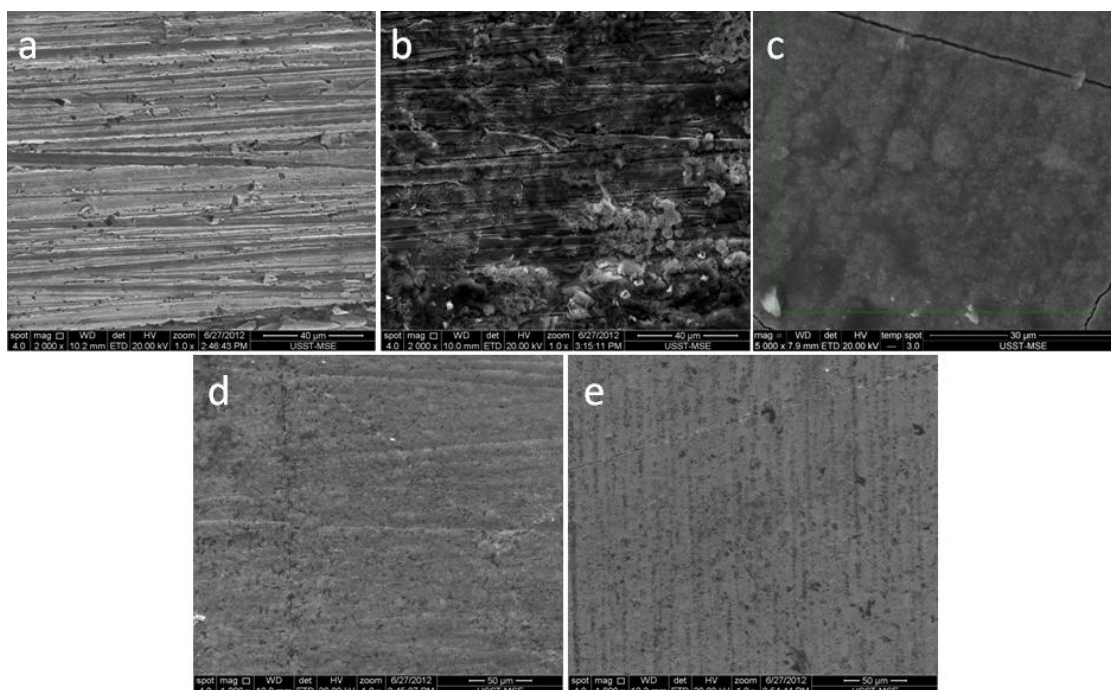


**Figure 3.** Surface morphology of FeCo films electrodeposited at different electrolyte pH. (a): pH=1; (b): pH=2; (c): pH=3; (d): pH=4; (e): pH=5.

#### 4. CONCLUSIONS

FeCo films were electrodeposited on Cu substrates at different electrolyte pH. The composition of FeCo films is greatly affected by the electrolyte pH. With increasing temperature, the Fe content is increased while Co content is decreased. Low electrolyte pH ( $\leq 3$ ) favors the formation of fcc  $\gamma$  phase while high electrolyte pH (4 and 5) leads to the formation of bcc  $\alpha$ -Co<sub>7</sub>Fe<sub>3</sub> phase in the studied films. High electrolyte pH leads to a small decrease in the lattice parameter for the fcc phase and a small increase for that of bcc phase. With increasing pH value, the averaged grain sizes of fcc phase and bcc phase increase. The films prepared at low pH values (1 and 2) shows a very poor quality with rough surface. The surfaces of the films electrodeposited at high pH value (3~5) are generally quite smooth, uniform and compact. And porous and cracks can be observed in the FeCo films electrodeposited at high pH value (3~5).

#### ACKNOWLEDGEMENTS

The present work was supported by National Natural Science Foundation of China (Grant No. 50901052, 51071109) and Program for Young Excellent Talents in Tongji University (Grant No. 2009KJ003) and “Chen Guang” project (Grant No.10CG21) supported by Shanghai Municipal Education Commission and Shanghai Education Development Foundation.

## References

1. I. Shao, L.T. Romankiw, C. Bonhote, *J. Cryst. Growth* 312 (2010) 1262
2. K. Sundaram, V. Dhanasekaran, T. Mahalingam, *Ionics* 17 (2011) 835
3. S. Mehrizi, M. Heydarzadeh Sohi, S.A. Seyyed Ebrahimi, *Surface & Coatings Technology* 205 (2011) 4757
4. W. Lu, P. Huang, C. He, B. Yan, *Int. J. Electrochem. Sci.* 7 (2012)12262
5. W. Lu, P. Huang, K. Li, P. Yan, Y. Wang and B. Yan, *Int. J. Electrochem. Sci.* 8 (2013)2354
6. W. Lu, P. Huang, C. He, B. Yan, *Int. J. Electrochem. Sci.* 8 (2013)914
7. Hakan Kockar, Mursel Alper, Turgut Sahin, Oznur Karaaga, *Journal of Magnetism and Magnetic Materials* 322 (2010)1095
8. J. A. R. Márquez, C. M. B. Rodríguez, C. M. Herrera, E. R. Rosa, O. Z. Angel, O. T. Pozos, *Int. J. Electrochem. Sci.* 6 (2011) 4059
9. Elizabeth Garfias-García, Mario Romero-Romo, María Teresa Ramírez-Silva, Manuel Palomar-Pardavé, *Int. J. Electrochem. Sci.* 7 (2012) 3102
10. A. Varea, E. Pellicer, S. Pané, B. J. Nelson, S. Suriñach, M. D. Baró and J. Sort, *Int. J. Electrochem. Sci.* 7 (2012) 1288
11. J.-W. Park, J.-Y. Eom, H.-S. Kwon, *Int. J. Electrochem. Sci.* 6 (2011) 3093
12. G. Orhan, G. Hapci, O. Keles, *Int. J. Electrochem. Sci.* 6 (2011) 3966
13. J.C. Ballesteros, E. Chainet, P. Ozil, Y. Meas, G. Trejo, *Int. J. Electrochem. Sci.* 6 (2011) 2632
14. H. Adelhani, M. Ghaemi, M. Ruzbehani, *Int. J. Electrochem. Sci.* 6 (2011) 123
15. H. Zhao, L. Liu, J. Zhu, Y. Tang, W. Hu, *Mater. Lett.* 61 (2007)1605
16. A. Mishra, A. Thakur, V. Srinivas, *J. Mater. Sci.* 44 (2009)352
17. F. Ebrahimi, Z. Ahmed, *J. Appl. Electrochem.* 33 (2003)733
18. S. Ullah, A. Badshah, F. Ahmed, R. Raza, A. Altaf, R. Hussain, *Int. J. Electrochem. Sci.* 6 (2011)3801
19. G. Orhan, G. Hapci, O. Keles, *Int. J. Electrochem. Sci.* 6 (2011)3966
20. Ting-Ruei Lee, Liuwen Chang, Chih-Hsiung Chen, *Surface & Coatings Technology* 207 (2012) 523
21. M. Saitou, S. Oshiro, S. M. Asadul Hossain, *J. Appl. Electrochem.* 38(2008) 309
22. A.M. Rashidi, A. Amadeh, *Surface & Coatings Technology* 204 (2009) 353
23. I. A. Carlos, M. R. H. Almeida, *J. Electroanal. Chem.* 562 (2004)153
24. G. Finazzi, E. Oliveira, I. Carlos, *Surface & Coatings Technology* 87 (2004) 377
25. L. Barbosa, M. Almeida, R. Carlos, M. Yonashiro, G. Oliveira, I. Carlos, *Surf. Coat. Technol.* 192 (2005) 145
26. V. Darrort, M. Troyon, J. Ebotht, C. Bissieux, C. Nicollin, *Thin Solid Films* 265 (1995) 52
27. V. Ganesh, D. Vijayaraghavan, V. Lakshminarayanan, *Appl. Surf. Sci.* 240 (2005) 28
28. T. Anik, M. Ebn Touhami, K. Himm, S. Schireen, R. A. Belkhamima, M. Abouchane, M. Cissé, *Int. J. Electrochem. Sci.* 7 (2012) 2009
29. L. Tian, J. Xu, S. Xiao, *Vacuum* 86 (2011) 27
30. X. Liu, P. Evans, G. Zangari, *IEEE Trans. Mag.* 36 (2000) 3479
31. S. Zhou, Q. Liu, D.G. Ivey, *IEEE Int. Nanoelectron. Conf.* 474 (2008) 4585531
32. R. Bertazzoli, D. Pletcher, *Electrochimica Acta.* 38 (1993) 671
33. H. Dahms, I.M. Croll, *J. Electrochem. Soc.* 112 (1965) 771
34. S. Hessami, C.W. Tobias, *J. Electrochem. Soc.* 136 (1989) 3611
35. T.M. Harris, J. St. Clair, *J. Electrochem. Soc.* 143 (1996) 3918
36. M. Matlosz, *J. Electrochem. Soc.* 140 (1993) 2272
37. B.C. Baker, A.C. West, *J. Electrochem. Soc.* 144 (1997) 169
38. N. Zech, E.J. Podlaha, D. Landolt, *J. Electrochem. Soc.* 146 (1999) 2892
39. H. Bakar, ASM Handbook, Volume 3 Alloy Phase Diagrams, ASM international, Materials Park,



Ohio (1992)

40. D. Zhou, M. Zhou, M. Zhu, X. Yang, M. Yue, *J. Appl. Phys.* 111 (2012) 07A319

41. S. H. Teh, I. I. Yaacob, *IEEE TRANSACTIONS ON MAGNETICS* 47 (2011) 4398

42. H. Kockar, M. Alper, T. Sahin, O. Karaaga, *Journal of Magnetism and Magnetic Materials* 322 (2010) 1095

© 2013 by ESG ([www.electrochemsci.org](http://www.electrochemsci.org))